ESTIMATION OF FAR-FIELD TSUNAMI POTENTIAL FOR THE CARIBBEAN COAST BASED ON NUMERICAL SIMULATION

Narcisse Zaibo[1], Efim Pelinovsky[2], Andrey Kurkin[3], and Andrey Kozelkov[3]

[1] Département de Physique, Université des Antilles et de la Guyane, Pointe-à-Pitre, France; email: narcisse.zahibo@univ-ag.fr
[2] Laboratory of Hydrophysics and Nonlinear Acoustics, Institute of Applied Physics, Nizhny Novgorod, Russia; email: enpeli@hydro.appl.sci-nnov.ru
[3] Applied Mathematics Department, State Technical University, Nizhny Novgorod, Russia; email: kurkin@kis.ru

ABSTRACT

The tsunami problem for the coast of the Caribbean basin is discussed. Briefly the historical data of tsunami in the Caribbean Sea are presented. Numerical simulation of potential tsunamis in the Caribbean Sea is performed in the framework of the nonlinear-shallow theory. The tsunami wave height distribution along the Caribbean Coast is computed. These results are used to estimate the far-field tsunami potential of various coastal locations in the Caribbean Sea. In fact, five zones with tsunami low risk are selected basing on prognostic computations, they are: the bay "Golfo de Batabano" and the coast of province "Ciego de Avila" in Cuba, the Nicaraguan Coast (between Bluefields and Puerto Cabezas), the border between Mexico and Belize, the bay "Golfo de Venezuela" in Venezuela. The analysis of historical data confirms that there was no tsunami in the selected zones. Also, the wave attenuation in the Caribbean Sea is investigated; in fact, wave amplitude decreases in an order if the tsunami source is located on the distance up to 1000 km from the coastal location. Both factors wave attenuation and wave height distribution should be taken into account in the planned warning system for the Caribbean Sea.

1. Introduction

The tsunami catalogue has been recently created for the Caribbean Sea (Lander et al, 2002; HTDB/ATL, 2002; Loughlin and Lander, 2003) and in particular, for the Lesser Antilles (Zahibo and Pelinovsky, 2001). In the past 500 years this region has had devastating tsunamis causing damage in many states of the Caribbean Basin. According to Lander et al (2002), totally, 91 reported waves might have been tsunamis. Of these, 27 are judged by the authors to be true, verified tsunamis and the additional nine are considered to be very likely true tsunamis. The list for the last century contains 33 events, thus one in every three years. Only for the last 35 years there were 6 true and almost true tsunamis: 1969, December 25 (earthquake with magnitude 7.6 in Lesser Antilles, maximal tsunami amplitude of 46 cm at Barbados); 1985, March 16 (moderate earthquake with magnitude 6.3 in Guadeloupe, several-centimeter tsunami was recorded at Basse Terre, Guadeloupe); 1989, November 1 (weak earthquake with magnitude 4.4 off the north coast of Puerto Rico generating a small wave in Cabo Rojo); 1991, April 22 (the earthquake with magnitude 7.6 created the tsunami that affected the coast of Central America from Costa Rica to Panama; wave height is 2 m in Cahuito Perto Viejo, Costa Rica); 1997, July 9 (the earthquake of magnitude 6.8 occurred off the coast of Venezuela and induced a weak tsunami on Tobago); 1997, December 26 (volcanic eruption in Montserrat generated the wave with height 3 m at Old Road Bay). The last tsunami occurred in Guadeloupe (Deshaies) at July 12, 2003 induced by the volcanic eruption in Montserrat (Zahibo et al, 2003a). Small boats moored in the mouth of the Deshaies River were carried on more than 60 meters, and some of them were damaged (the sea rised on 50 cm approximately).

Tsunami phenomenon in the Caribbean Sea has been the subject of special study in recent years. First of all, we would like to mention the calculation of the tsunami travel time charts for the Caribbean (Weissert, 1990). The estimated time for a complete crossing of the Caribbean is 3.2 hrs laterally and 1.5 hrs meridionally. Two historical events in the Caribbean, the 1918 Puerto Rico tsunami and the 1867 Virgin Island tsunami, induced by the davastating earthquakes, have been simulated by Mercado & McCann (1998) and Zahibo et al (2003b). Computed values of the tsunami wave heights are in a satisfactory agreement with the observed data. The propagation of the trans-atlantic tsunami after the catastrophic Lisbon earthquake (01/11/1755) has been modelled by Mader (2001a). According to his calculations, the wave amplitude east of Saba (Lesser Antilles) is 5 m close to the observed value (7 m).

Heinrich et al (2001) performed the numerical simulation of the 26/12/1997 debris avalanche in Montserrat (Lesser Antilles) that induced tsunami waves up to 3 m.

Taking into account the lack of historical data for the evaluation of the tsunami risk in the Caribbean Sea, the simulation of possible tsunamis can be an effective tool to forecast tsunami events in the future. The potential hazard on the northern coast of Puerto Rico due to submarine landslides along the Puerto Rico Trench has been estimated (Mercado et al, 2002). We would also like to mention the possible tsunami expected from a lateral collapse of the Cumbre Vieja Volcano on La Palma (Canary Islands); according to Mader (2001b) its height may be 3 m high on the Caribbean Islands (Saba Island). Ward & Day (2001) and Pararas-Carayannis (2002) discusses 20-40 m waves during this event in the Caribbean. Heinrich et al (1998, 1999) studying the danger of the volcanic eruption in the Soufriere Hills Volcano, Montserrat, showed that the potential debris avalanche can induce the tsunami waves of 1-2 m in the nearest zone and 50 cm at Guadeloupe and Antigua. Le Friant et al (2002, 2003) simulated the tsunami waves from the potential eruptions of some volcanos in the Lesser Antilles (Martinique, Dominica) and showed that the islands in the Lesser Antilles face a non-negligible risk from generation of tsunamis associated with potential future events.

The present paper has a goal to estimate the far-field tsunami potential for the Caribbean Sea basing on the numerical simulation of the prognostic events. The historical information of tsunamis in the Caribbean Sea with intensity exceeded 2 on the Imamura-Soloviev scale is briefly reproduced in section 2. The numerical simulation of prognostic tsunamis is performed with the use of the TUNAMI code that is based on the nonlinear shallow-water theory. The important problem of prognostic tsunami sources is discussed in section 3. Additionally to the small number of the seismic sources, the hydrodynamic sources are selected almost uniformly along the coast of the Caribbean Sea. The computed distributions of tsunami heights along the Caribbean Coast are described in section 4. These distributions are used for preliminary estimations of the tsunami risk (far-field tsunami potential) in the Caribbean Sea. The five zones with tsunami low risk are selected based on prognostic computations; they are, “Golfo de Batabano” and coast of province “Ciego de Avila” in Cuba, Nicaraguan coast (between Bluefields and Puerto Cabezas), border between Mexico and Belize, “Golfo de Venezuela” in Venezuela. The analysis of historical data confirms that there was no tsunami in the selected zones. The computed wave attenuation in the Caribbean Sea is investigated in section 5. If the tsunami sources are located on the distance above 1000 km from the coastal locations such far-field tsunamis can be evaluated as the low-risk tsunamis.

2. Intense historical tsunamis in the Caribbean Sea

Most of tsunamis in the Caribbean Sea have been generated by the underwater earthquakes that occurred in the Caribbean. The seismicity of the Caribbean basin is high, see Figure 1 taken from HTDB/ATL (2002). A few of tsunamis are the distant tsunami that came from the Atlantic coast of Europe. Some local tsunamis were caused by the volcano eruptions; most of volcanos are located on the Lesser Antilles. Several tsunamis described in catalogues are of an unknown origin; perhaps, they are hurricane storm surges. The geographical distribution of tsunamis with various intensities on the Imamura-Soloviev scale is shown in Figure 2. The intensity tsunamis in the Caribbean Sea did not exceed 3.0 (mean height 4-8 m on the coastal line of 200-400 km). The list of tsunamis with intensity 2.0-3.0 is given in Table 1 extracted from HTDB/ATL (2002); it includes 27 events. The return period of such intense tsunamis is about 15-20 years. Taking into account that the last tsunami with intensity 2 was recorded in 1979; we may point out that the probability of the next tsunami in the nearest future in the Caribbean Sea is high.

Meanwhile, to evaluate the tsunami risk for coastal locations in the Caribbean Sea basing on the historical data only is a very difficult task due to the lack of quantitative information. The modeling of the several historical events in the Caribbean Sea that occurred in 1755, 1867, 1918 and 1997 (Mader, 2001a; Zahibo et al, 2003b; Mercado & McCann, 1998; Heinrich et al, 2001) and the satisfactory agreement with observations demonstrate the applicability of existing mathematical theories to describe the tsunami characteristics. Taking into account the historical data and numerical simulations the variability of wave heights along the coastal line is very large due to the local features of the coastal topography and the directivity of tsunami sources. By using possible locations of tsunami sources (seismic zones, volcano locations and so on) the synthetic catalogue of possible tsunamis at the fixed coastal locations can be created; this will allow to compare the tsunami risk for different areas. This approach is now very popular for estimations of far-field tsunami potential when the tsunami sources are located in the open sea (Go et al, 1988; Nagano et al, 1991; Mofjeld et al, 2001; Choi et al, 2001, 2002a; Yalciner et al, 2002; Koike et al, 2003; Sato et al, 2003), and here it will be applied for the Caribbean Sea.

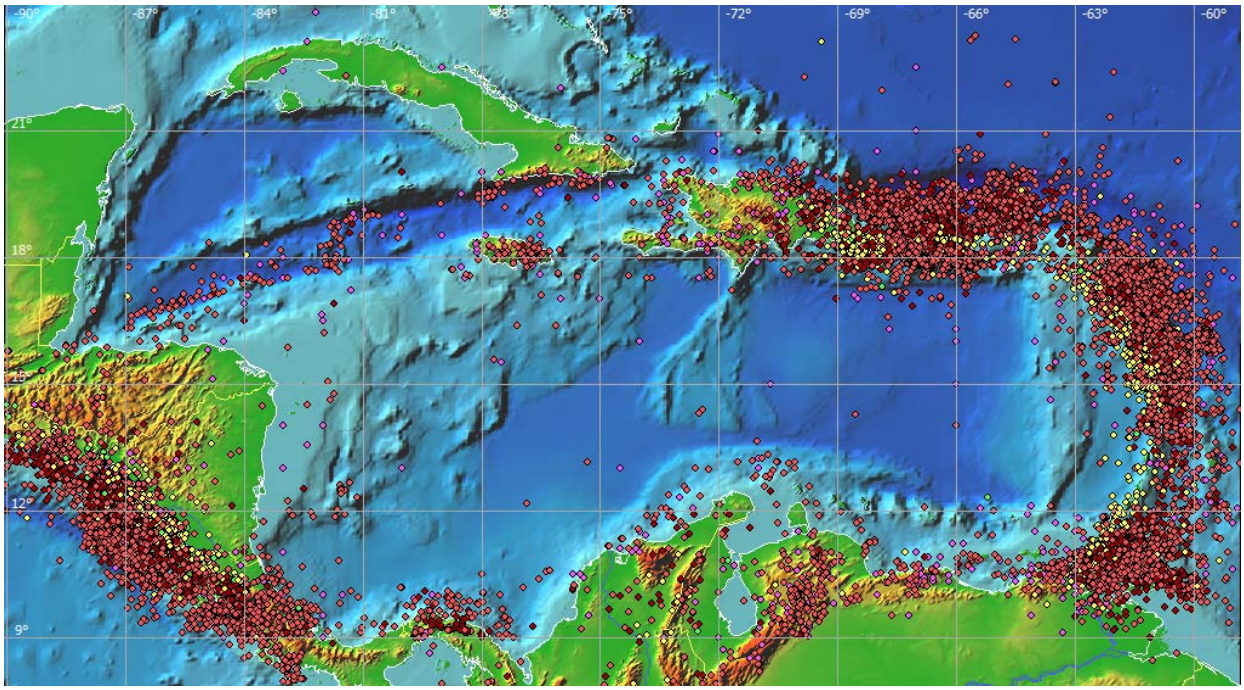

Figure 1. Seismicity of the Caribbean Sea

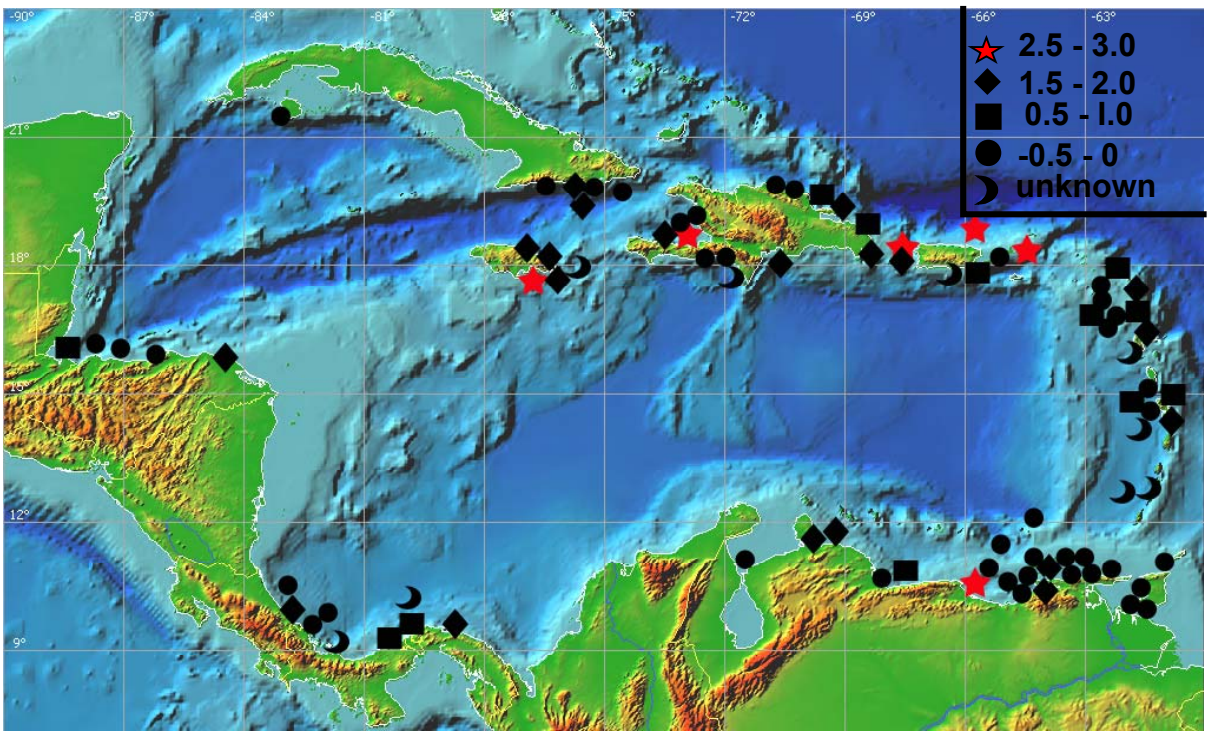

Figure 2. Historical tsunami distribution in the Caribbean Sea (numbers – tsunami intensity)

Table 1. List of tsunamis with intensity 2-3 in the Caribbean Sea

(*Ms* is the surface magnitude, *I* is the tsunami intensity and H_{max} is the maximum wave height)

Date	Lat	Lon	Ms	I	H_{max} (m)	Source
01.09.1530	10.7	-64.1	7	2	7,3	Peninsula de Paria, Cuba
01.09.1543	10.6	-64.1	7	2		Cumana, Venezuela
01.03.1688	17.6	-76.7		2		Port Royal, Jamaica
16.04.1690	17.5	-61.5	8	2		Charlotte Amalie, US Virgin Is.
07.06.1692	17.8	-76.7	7	3	10	Port Royal, Liganee, Jamaica
18.10.1751	18.5	-70.7	7	2		Azua de Compostela, Haiti
21.11.1751	18.5	-73.5	7	2	7	St Martin, Antigua, Martinique
11.06.1766	20	-75.5	7	2		Jamaica
03.10.1780	18.1	-78.1	7	2	3,2	Savanna la Mar, Jamaica
28.03.1787	19	-66	8	2,5	4	S. Mexico
05.05.1802	10	-60		2		Rio Orinoko, Cumana, Venezuela
26.03.1812	10.3	-64.1		2		La Guaira, Venezuela
11.11.1812	18	-76.5		2		Annotto Bay, Jamaica
30.11.1823	14.2	-61.1		2		St Pierre, Martinique
30.11.1824	14.5	-61		2		St Pierre, Martinique
07.05.1842	18.5	-72.5	7.7	3	8,3	Hispaniola, Haiti
17.07.1852	19.5	-75.5		2		Santiago de Cuba, Cuba
09.08.1856	15.8	-84.3		2	5	Rio Patuca, Honduras
18.11.1867	18.4	-64.3	7.5	3	10	St Thomas, Virgin Is.
29.10.1900	10.3	-65.9		3	10	Puerto Tay, Venezuela
14.01.1907	18.2	-76.7	7	2	9,1	Annotto Bay, Jamaica
11.10.1918	18.5	-67.5	7.5	2,5	6	Aguadilla, Puerto Rico
04.08.1946	19.25	-69	8	2	4,7	Hispaniola, Dominican Republic
02.12.1951	13.5	-60		2		Puerto Rico and Barbados
17.08.1952	18.4	-68.4		2		Puerto Rico, Dominican Rep,
18.01.1955	11.3	-69.4	5.5	2		La Vela, Venezuela
03.09.1979	11.5	-69.3		2		Puerto Cumaredo, Venezuela

3. Numerical Model and Potential Tsunami Sources

To describe the tsunami wave propagation in the Caribbean Sea, the nonlinear shallow water theory in the Cartesian coordinates is used. Due to the lowest latitude of the Caribbean, the Coriolis effect is neglected. These equations are,

$$\frac{\partial M}{\partial t} + \frac{\partial}{\partial x}\left(\frac{M^2}{D}\right) + \frac{\partial}{\partial y}\left(\frac{MN}{D}\right) + gD\frac{\partial \eta}{\partial x} + \frac{k}{2D^2}M\sqrt{M^2 + N^2} = 0\,, \qquad (1)$$

$$\frac{\partial N}{\partial t} + \frac{\partial}{\partial x}\left(\frac{MN}{D}\right) + \frac{\partial}{\partial y}\left(\frac{N^2}{D}\right) + gD\frac{\partial \eta}{\partial y} + \frac{k}{2D^2}N\sqrt{M^2 + N^2} = 0\,, \qquad (2)$$

$$\frac{\partial \eta}{\partial t} + \frac{\partial M}{\partial x} + \frac{\partial N}{\partial y} = 0\,, \qquad (3)$$

where η is sea level displacement, t is time, x and y are horizontal coordinates in zonal and meridional directions, M and N are discharge fluxes in horizontal plane along x and y coordinates, $D = h(x,y) + \eta$ is the total water depth, $h(x,y)$ is unperturbed basin depth, g is the gravity acceleration and $k = 0.0025$ is the typical value for the bottom friction coefficient.

Numerical simulations used the tsunami propagation model Tunami-N2 that was developed in Tohoku University (Japan) and provided through the Tsunami Inundation Modeling Exchange (Time) program, see Goto el al., (1997). It has been applied to several case studies in the Caribbean Sea (Mercado & McCann, 1998; Zahibo et al, 2003). The model solves the governing equations by the finite difference technique with the leap-frog scheme (Goto *et al*., 1997). The bathymetry of the Caribbean Sea was obtained from the Smith and Sandwell global seafloor topography (Etopo2) with a 3 km grid size. The time step is selected as 6 sec to satisfy the stability condition. The total number of grid points in the study area is 568568 (1001×568). Along the depth of 20 m contour line the vertical wall boundary condition is assumed. Free outward passage of the wave is permitted at the open sea boundaries.

Our goal is to estimate the far-field tsunami potential for the Caribbean Sea by creating the synthetic catalogue of possible tsunami generating in the open sea. Such sources are of seismic origin, and they will be analyzed for tsunami prediction. First of all, the synthetic catalogue should include the sources of the historical large tsunamis (with intensity exceeded

1 as minimum). We use only events with the knowen characteristics of their origin (coordinate, magnitude, maximum wave height), these 19 events are summarized in Table 2 taken from HTDB/ATL (2002); their epicenters are shown in Figure 3. The fault line (axis of the initial tsunami displacement) is assumed to be parallel to the isobath. Since there is no sufficient information available about the source parameters of the earthquake they are chosen as followed: length of the fault is 120 km, width is 30 km; dip and slip angles of the fault are selected as 70^0 and 90^0 respectively. The displacement has been selected as 8 m. The focal depth has been taken from the catalogue or 3000 m if there is no such information. These parameters have been used to simulate the 1867 Virgin tsunami, one of the most destructive tsunamis in the Caribbean basin (Zahibo et al., 2003b).

The initial wave ("of seismic origin") is computed according to Okada (1985), its characteristic form is shown in Figure 4a. The depression of the water surface is on the deepest part of the sea. The elevation of the sea level in the source is about 4 m, and the depression is 2 m in average.

Additionally, the "hydrodynamic" sources presented by pyramidal displacements with the height of 5 m and the diameter of 50 km (Figure 4b) and distributed almost uniformly in the basin of the Caribbean Sea (Figure 5) are included in the synthetic catalogue. The total number of the "hydrodynamic" sources is 102 and they may demonstrate the influence of the topography features on the wave propagation in the "pure form" because the hydrodynamic source has the almost isotropic directivity.

Wave propagation from each "seismic" and "hydrodynamic" source is computed and the wave characteristics are collected for each coastal location at the Caribbean Sea. This model was used particularly to model the 1867 Virgin tsunami (Zahibo et al., 2003b). The computed directivity diagram is presented in Figure 6. It is clearly seen that the wave height is non-uniform along the coast of the Caribbean Sea: tsunami is significant in the epicentral area (Virgin Islands, Puerto Rica), and also on the northern and southern Lesser Antilles, but not in the central part of the Lesser Antilles. This non-uniformity of tsunami distribution is confirmed by the observed data (Zahibo et al., 2003b). Figure 6 shows also the existence of the "gaps" in wave characteristics, in particular, wave amplitude is negligibly weak on Cuba, Panama and Nicaragua. The same computing is done for total 121 prognostic events. The analysis of these data allows to estimate the far-field tsunami potential of various areas in the Caribbean Basin.

Table 2. Chosen parameters of tsunamigeneric historical earthquakes

Date	Lat	Lon	Magnitude	Intensity	H_{max}, m
01.09.1530	10.70	-64.10	7.0	2.0	7.3
07.06.1692	17.80	-76.70	7.0	3.0	10.0
21.11.1751	18.50	-73.50	7.0	2.0	7.0
03.10.1780	18.10	-78.10	7.0	2.0	3.2
28.03.1787	19.00	-66.00	8.0	2.5	4.0
07.05.1842	18.50	-72.50	7.7	3.0	8.3
08.02.1843	16.50	-62.20	8.3	1.0	1.2
09.08.1856	15.80	-83.30	-	2.0	5.0
18.11.1867	18.00	-65.00	7.5	3.0	10.0
17.03.1868	18.40	-64.90	7.0	1.0	0.6
07.09.1882	9.50	-78.70	7.9	1.5	3.0
29.10.1900	10.30	-65.90	-	3.0	10.0
14.01.1907	18.20	-76.70	7.0	2.0	9.1
26.04.1916	9.20	-83.10	7.5	1.0	1.2
11.10.1918	18.50	-67.50	7.5	2.5	6.0
24.10.1918	18.50	-67.50	-	1.5	2.6
04.08.1946	19.25	-69.00	8.0	2.0	4.7
22.04.1991	9.60	-83.20	7.6	1.5	3.0
26.12.1997	16.70	-62.20	-	1.0	3.0

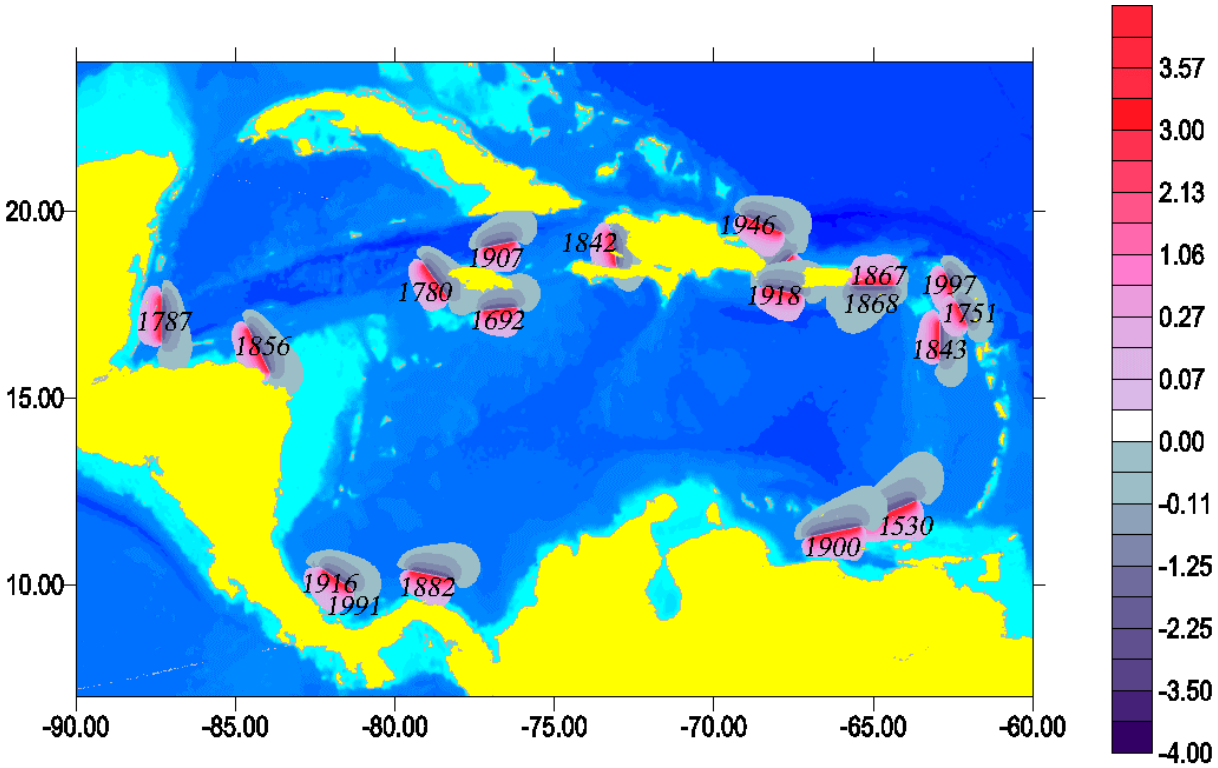

Figure 3. Epicenters of historical tsunamis used in numerical simulation

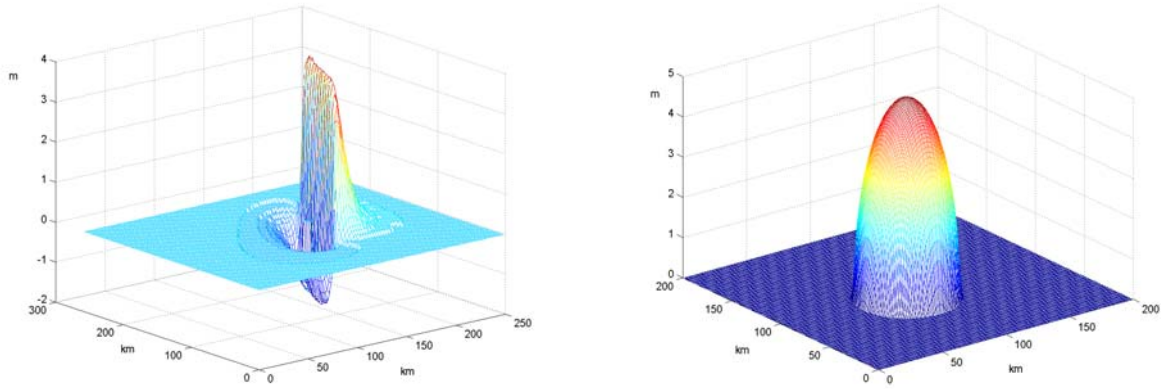

a) *b*)

Figure 4. Initial wave shapes: a) “seismic” source, b) “hydrodynamic” source

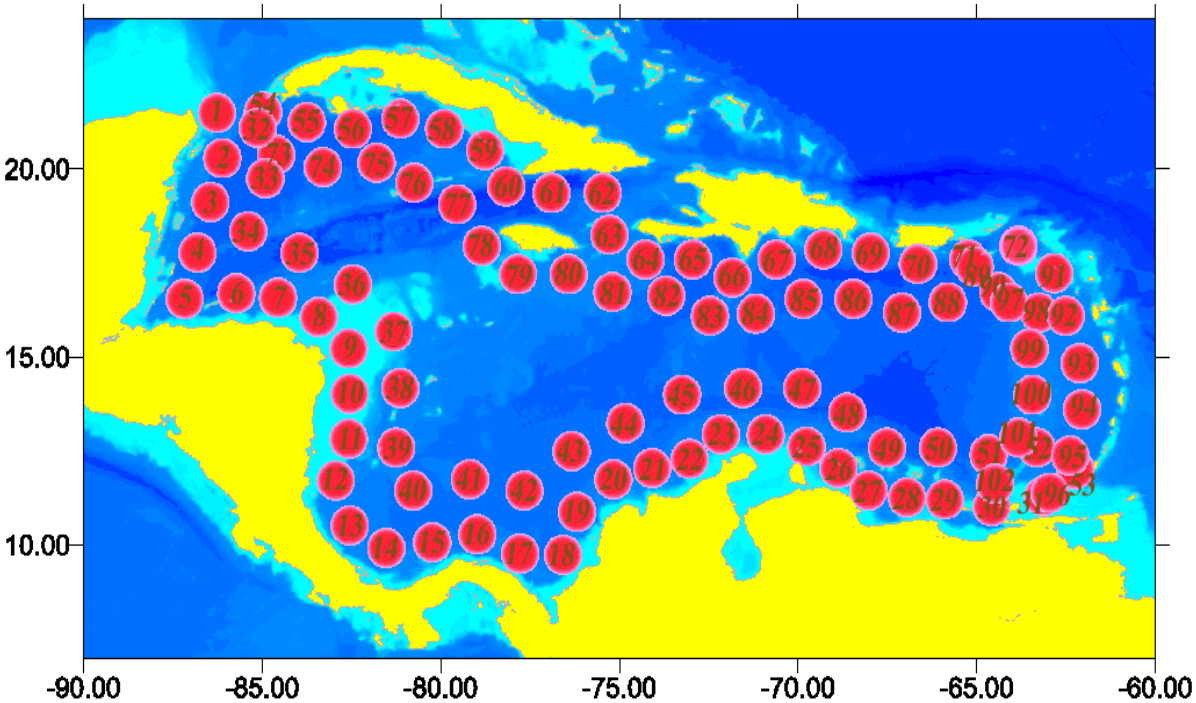

Figure 5. Locations of the “hydrodynamic” sources in the Caribbean Sea

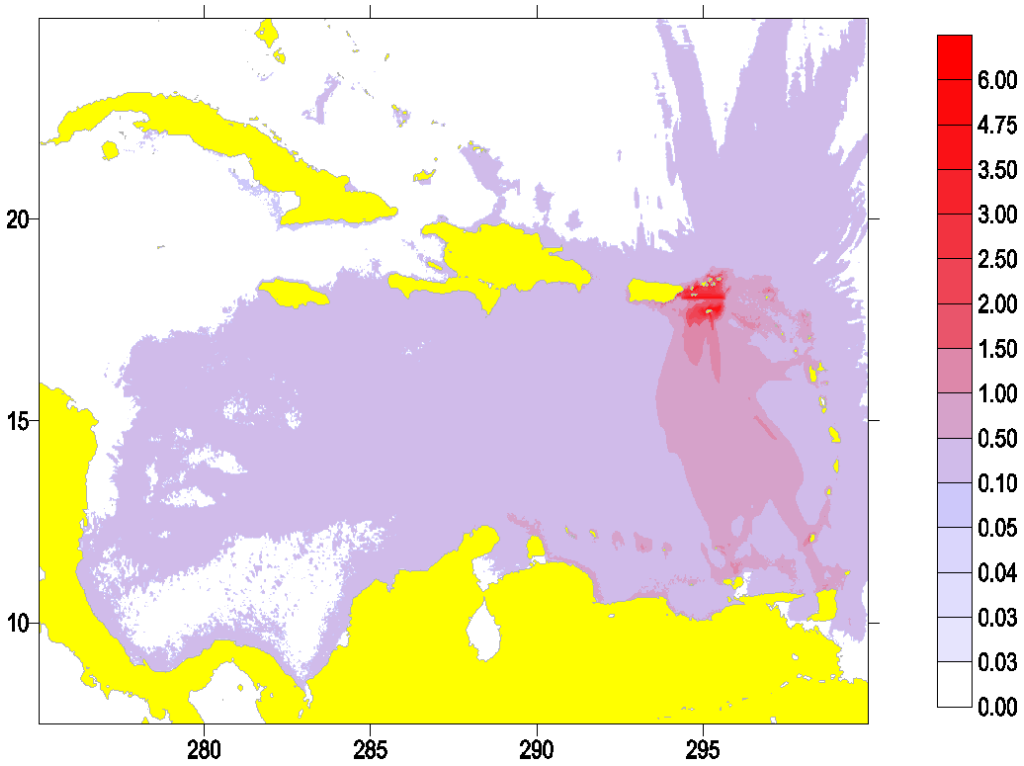

Figure 6. The distribution of maximum crest amplitude in the Caribbean Sea (1867 event)

4. Computed wave height distribution along the coast of the Caribbean Sea

For the analysis of the tsunami characteristics for various coastal areas, the Caribbean Sea is conditionally divided into several "geographic" zones (Figure 7). They are: the Great Antilles excepting Jamaica (zone A), Jamaica (zone B), the Lesser Antilles (zone C), and the Caribbean coast of the Central and South America (zone D). Time series of the sea displacement are calculated for 3467 points near the coast (last sea points in numerical grid), their numeration is also shown in Figure 7. The distance between such points is the mesh size, 3 km. It is important to mention that we use the "vertical wall" boundary condition at the depth 20 m, so the wave runup on the beach of the real configuration is not included. The results of our calculations of the wave height near the "vertical wall" (at depths 20-150 m) can be used in the future for the detailed investigation of the tsunami runup height within coastal locations.

First of all, the distribution functions of the wave heights for each event are computed. As it is expected, the distribution function of the wave heights along the coast is described well by the log-normal curve (Choi et al, 2002b)

$$F(H) = \frac{1}{\sqrt{2\pi}\ln 10\sigma}\int_H^{\infty}\exp\left(-\frac{(\log h - a)^2}{2\sigma^2}\right)\frac{dh}{h}, \tag{4}$$

where a = <*log H*> is the average value of the wave height logarithm, and σ is the standard deviation of the height logarithm. The results of the computing of the distribution function for modeled destructive tsunami 18.11.1867 that occurred after the strong earthquake on the Virgin Islands are demonstrated on Figure 8.

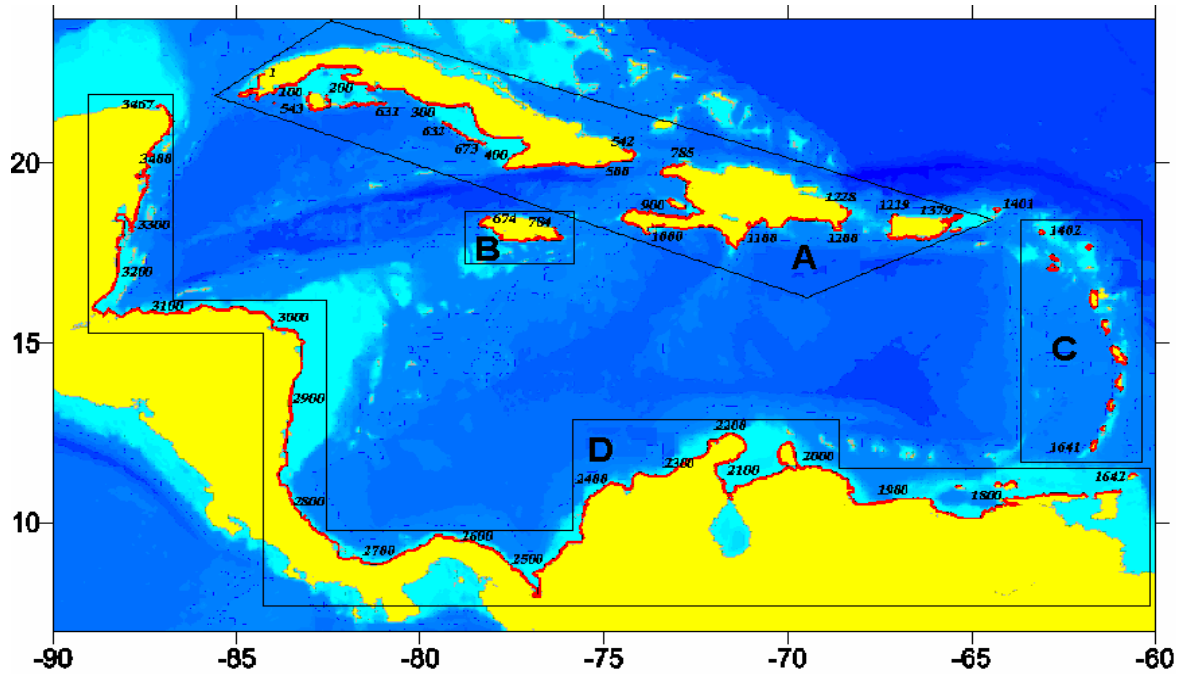

Figure 7. Selected zones in the Caribbean Sea (numbers – computed "tide-gauges" located in the last sea grid points)

The computed maximum values of positive (crest) and negative (trough) wave amplitudes in each zones calculated for the "seismic" events are summarized in Table 3. This Table illustrates the "trans-sea" character of tsunami propagation, and large tsunamis should be felt on many coastal locations of the Caribbean Sea. Historical data of the 1867 Virgin Island tsunami confirm this conclusion; this tsunami has been felt on many islands of the Caribbean: Puerto Rico, Virgin Islands, St Kitts, Antigua, Guadeloupe, Grenadines, Grenada, Isle de Margarita (Venezuela). The results of the numerical simulation of the 1867 tsunami are in reasonable agreement with the observation data (Zahibo et al, 2003). Due to the lack of historical data and tsunami source for other events we will not discuss here the computed results for the "seismic" event.

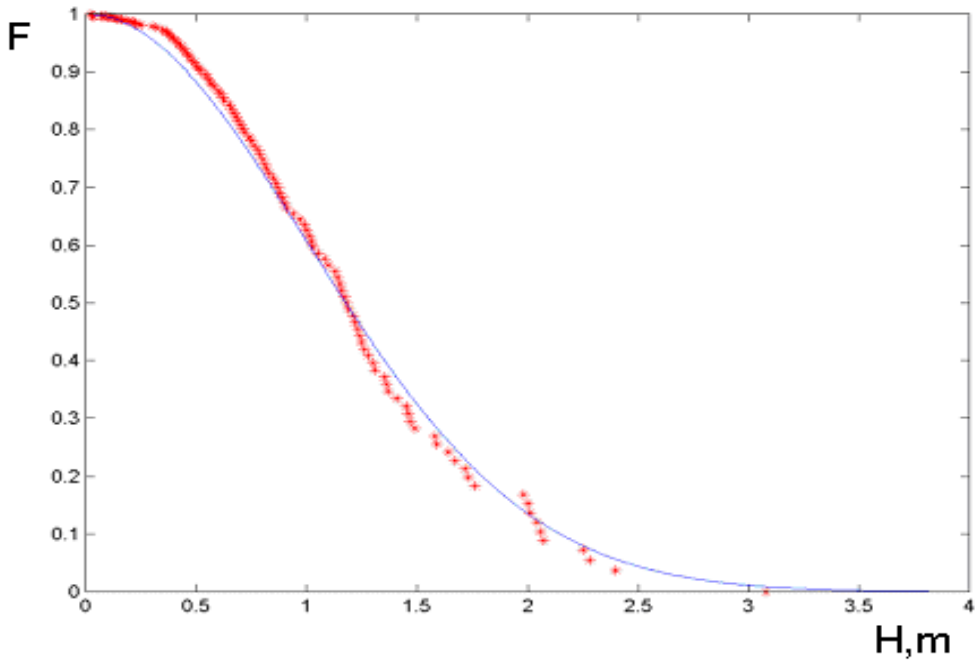

Figure 8. Computed distribution function (points) and its log-normal approximation (solid line) for the 1867 Virgin Island tsunami

Table 3. Computed maximum values of positive and negative amplitudes for "seismic" sources

Date	Zone A		Zone B		Zone C		Zone D	
	H_{max}	H_{min}	H_{max}	H_{min}	H_{max}	H_{min}	H_{max}	H_{min}
01.09.1530	4.11	-3.26	0.60	-0.6	3.41	-3.07	4.12	-7
07.06.1692	1.39	-1.33	5.96	-5.1	0.94	-1	2.79	-1.96
21.11.1751	1.84	-2.59	0.24	-0.2	2.89	-4.06	0.64	-0.57
03.10.1780	2.19	-1.45	3.92	-2.9	0.41	-0.45	0.88	-0.79
28.03.1787	1.91	-1.93	0.88	-0.6	0.16	-0.17	2.29	-2.56
07.05.1842	4.67	-6.14	2.94	-3.1	0.26	-0.25	0.82	-0.70
08.02.1843	1.34	-1.33	0.53	-0.4	1.86	-1.17	0.79	-1.06
09.08.1856	1.21	-0.7	0.55	-3.1	0.11	-0.25	2.95	-6.14
18.11.1867	5.34	-3.68	0.50	-0.5	2.66	-4.40	1.02	-1.12
17.03.1868	0.48	-0.27	0.11	-0.1	0.61	-0.62	0.13	-0.1
07.09.1882	1.67	-1.60	1.57	-1.6	0.54	-0.62	2.73	-2.84
29.10.1900	1.83	-1.81	0.68	-0.8	1.21	-1.20	5.05	-6.78
14.01.1907	7.75	-8.02	3.77	-5.3	0.45	-0.37	1.14	-1.16
26.04.1916	0.31	-0.23	0.86	-0.4	0.21	-0.12	0.92	-0.54
11.10.1918	6.12	-6.50	0.54	-0.6	1.07	-1.02	0.83	-0.78
24.10.1918	2.21	-2.21	0.77	-0.7	1.15	-1.11	0.75	-0.68
04.08.1946	3.36	-3.46	0.23	-0.2	0.35	-0.33	0.25	-0.28
22.04.1991	1.01	-0.99	1.13	-0.8	0.29	-0.34	2.96	-2.15
26.12.1997	1.65	-0.84	0.34	-0.3	2.71	-2.88	0.66	-0.68

Taking into account that the number of the «seismic» events is not too much, the detailed analysis of the wave height distributions is done for the 102 «hydrodynamic» sources. Our goal is to study the far-field tsunami potential; so we investigate wave characteristics in the fixed zone (for instance, A) using the sources in other zones (in this example, in zones B, C, and D). Each distribution of the crest amplitude along the coast is normalized on its maximum value to eliminate the difference in the intensity due to the different distance of the «hydrodynamic» sources to the coast. These distributions (normalized crest amplitude) are presented in Figure 9. Numbers on the horizontal axis correspond to the numbers of computed «tide-gauges» on Figure 7. It is clearly seen, that wave distributions have gaps with weak relative amplitudes (less than 0.1) which do not depend on the location of the tsunami source (vertical arrows show the locations of such gaps). The existence of areas with low wave amplitudes is related to the local features of the bottom and coastal topography. Therefore, we may call these areas as zones with the low tsunami risk. All far-field tsunamis in such areas will be weak and will not induce the significant impact on the coast. The prediction of zones with low risk by using the hydro-modelling only is the main result of the given study.

Geographical distribution of the selected zones with low tsunami risk (stars) with respect to the far-field tsunamis originating in the Caribbean Sea is shown in Figure 10. In such zones the relative wave height does not exceed 0.1 from all far sources. First of all, two zones can be selected on Cuba: Bay "Golfo de Batabano" protected from far-field tsunamis by the islands "Isla de la Juventud" and the Caribbean coast of the province "Ciego de Avila" protected by "Archipielago de los Jardinas de la Reina". These zones are protected from tsunamis originating in Central and South America and the Lesser Antilles. Two other zones are located on the Caribbean coast of Central America: near the border between Mexico and Belize, and the Nicaraguan coast (between Bluefields and Puerto Cabezas). The last, fifth zone is located on the Venezuelan coast (Bay "Golfo de Venezuela"); this bay is protected by the Aruba (the Netherlands Antilles). Zones with low tsunami risk located in Central and South America are protected from tsunamis originating in the Great and Lesser Antilles. The analysis of historical tsunamis that occurred in the Caribbean Sea (Figure 2) confirms that there was no tsunami in the computed zones of low tsunami risk.

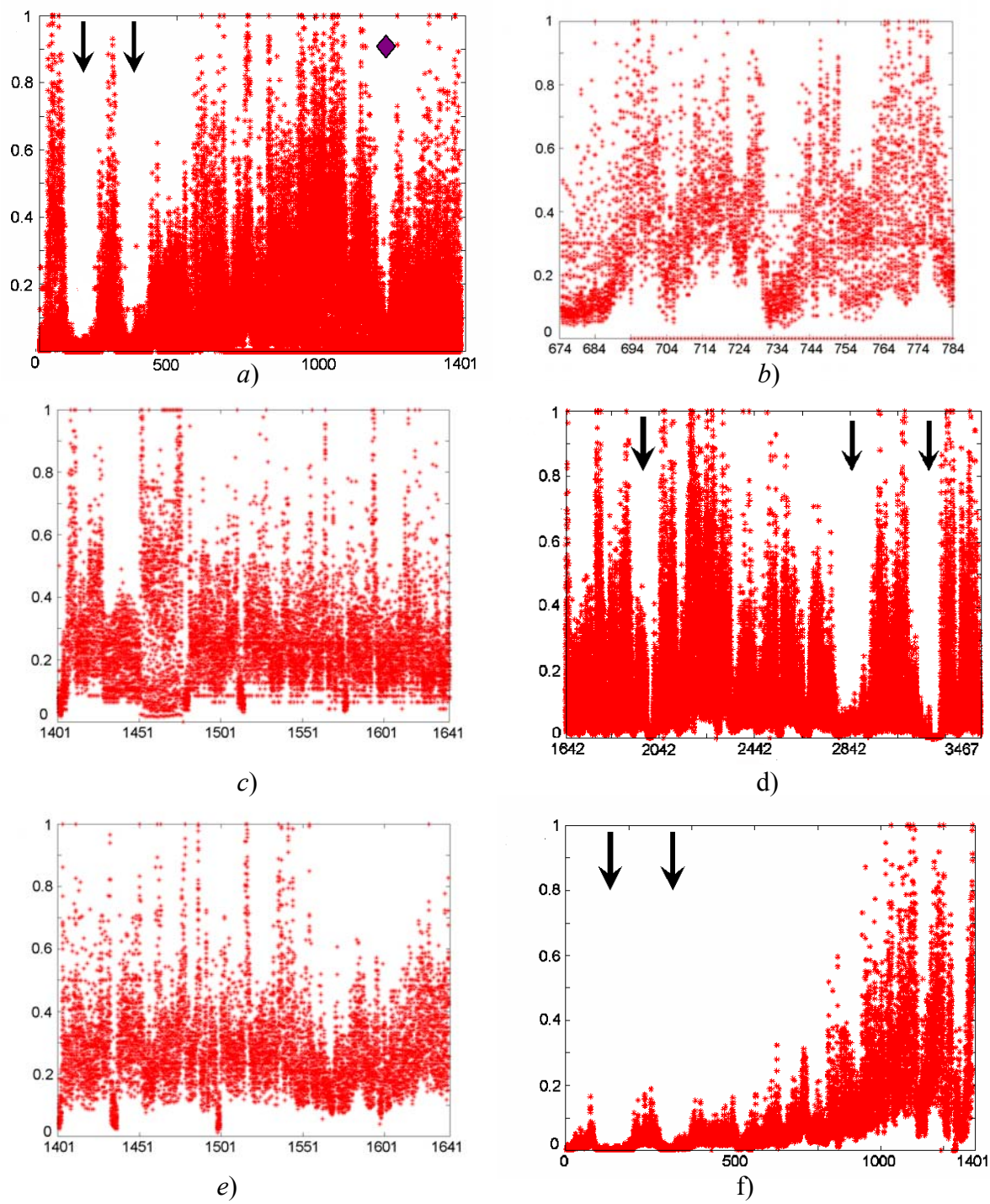

Figure 9. Normalized crest amplitude distribution for various zones
a) zone A, sources in zone D, b) zone B, sources in zone D, c) zone C, sources in zone D, d) zone D, sources in zones A and B, e) zone C, sources in zones A and B, f) zone A, sources in zone C, g) zone B, sources in zone C, and h) zone D, sources in zone C

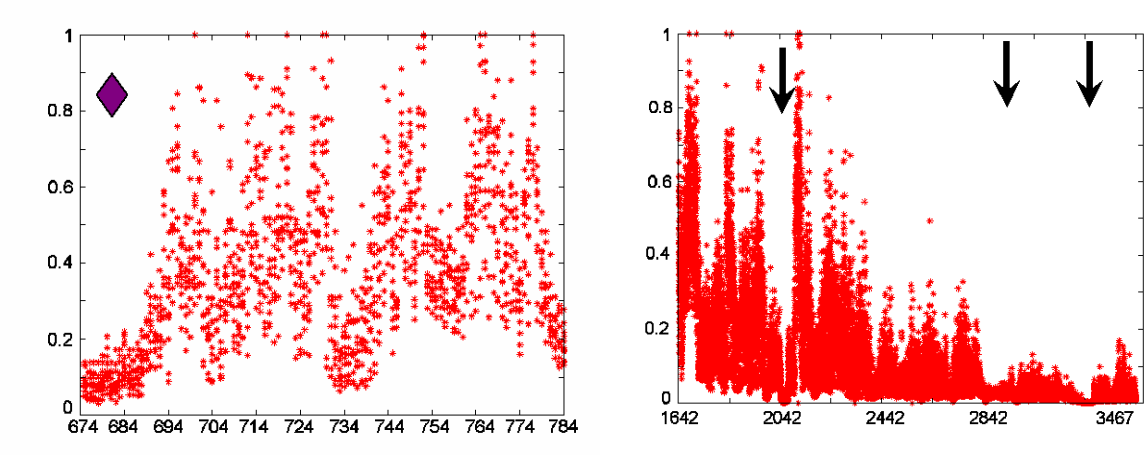

g) h)

Figure 9. Normalized crest amplitude distribution for various zones (continued)
b) zone A, sources in zone D, b) zone B, sources in zone D, c) zone C, sources in zone D, d) zone D, sources in zones A and B, e) zone C, sources in zones A and B, f) zone A, sources in zone C, g) zone B, sources in zone C, and h) zone D, sources in zone C

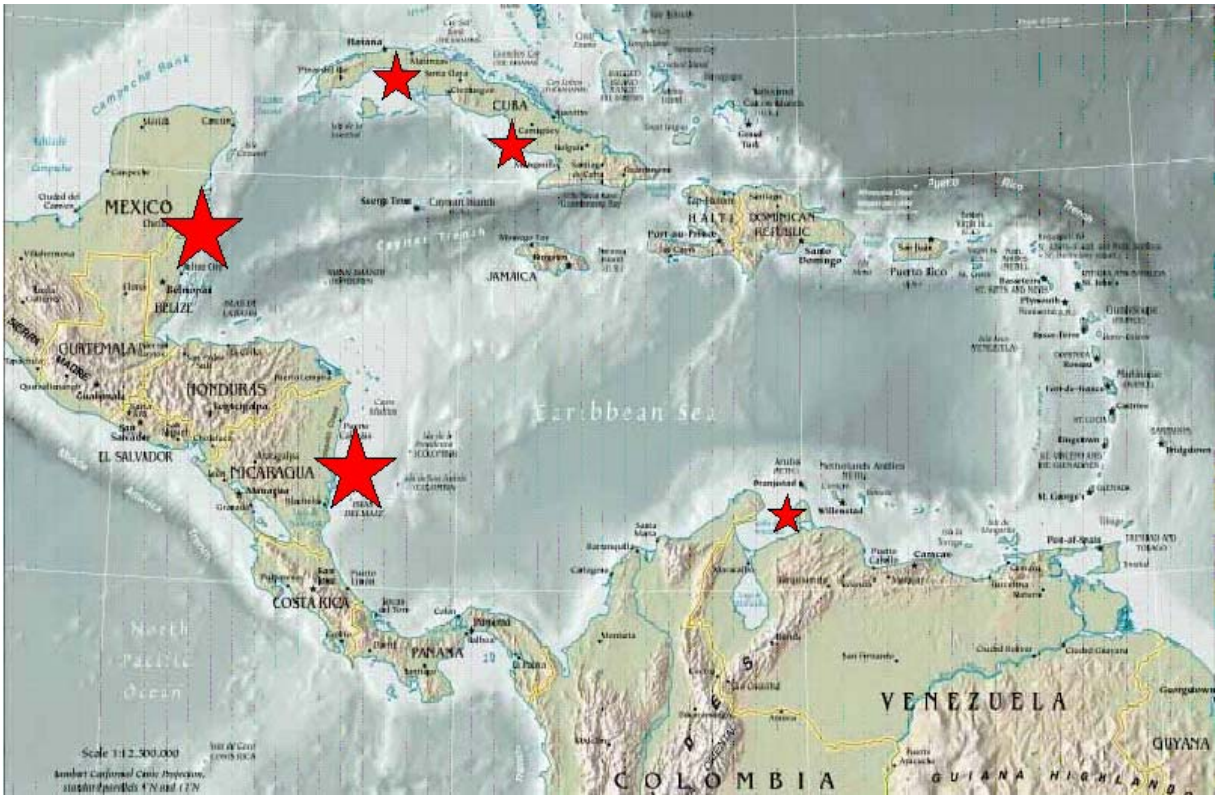

Figure 10. Geographical distribution of the zones with low tsunami risk (stars) in the Caribbean Sea

Some coastal locations are protected from part of far-field tsunamis only (they are indicated by rhombi on wave distribution in Figure 9). For instance, the eastern coast of Dominican Republic is protected from tsunamis originating in the Central and South America. The western coast of Jamaica and the western part of Cuba are protected from tsunamis originating from the Lesser Antilles. In fact, the whole coast of Central America (from Costa Rica to Mexico) is protected from tsunamis generating in the Lesser Antilles. Non-uniformity in the tsunami wave height distribution from far-field tsunamis should be used for the planned tsunami warning system for the Caribbean Sea.

5. Wave attenuation in the Caribbean Sea

Geographic distribution of the wave height allows to compare the protection of the various coastal locations from tsunamis with the sources arbitrary distributed in the Caribbean Sea. Another important factor influencing the tsunami risk is the distance to the possible tsunami-genetic zones. Figure 11 shows the computed wave height at Deshaies (the northern point of Guadeloupe, where the wave height during the 1867 Virgin tsunami reached 10 m) and at St George's (Grenada) as the functions of the distance to all 102 hydrodynamic sources. Taking into account that the water displacement in the hydrodynamic source has the same parameters (height, H_e = 5 m, and diameter, D = 50 km), these functions characterise the influence of the bottom topography on the wave attenuation. On the distance up to 1000 km these functions can be approximated by the polynomial curve

$$\frac{H(r)}{H_e} = 2\left(\frac{r}{D}\right)^{-\alpha} , \qquad (5)$$

where r is the distance from the source to Deshaies and α is the attenuation ratio. Factor 2 is inserted in the formula (5), because the wave height at Deshaies is computed with the boundary condition «vertical wall» at the last sea point; in this case the wave height at the wall is twice more than the height of the incident wave. Two approximations with $\alpha = 2/3$ and $\alpha = 1$ are presented in Figure 11 by the dash and solid lines consequently. We should also point out that the slope of approximated curves exceeds $\alpha = ½$ characterising the linear long waves in the basin of constant depth. The strongest attenuation typical of the dispersive tsunamis is related to the bottom irregularities only (not to bottom depth as in Boussinesq and Korteweg – de Vries equations). Such dispersion is manifestated, for instance, for along-

coastal propagation of the waves as the edge waves. The wave height is attenuated in an order on distances about 1000 km and, therefore, tsunami risk becomes low if the possible tsunami source is too far from the coastal locations. This important conclusion should be taken into account for the planning warning system for the Caribbean Sea.

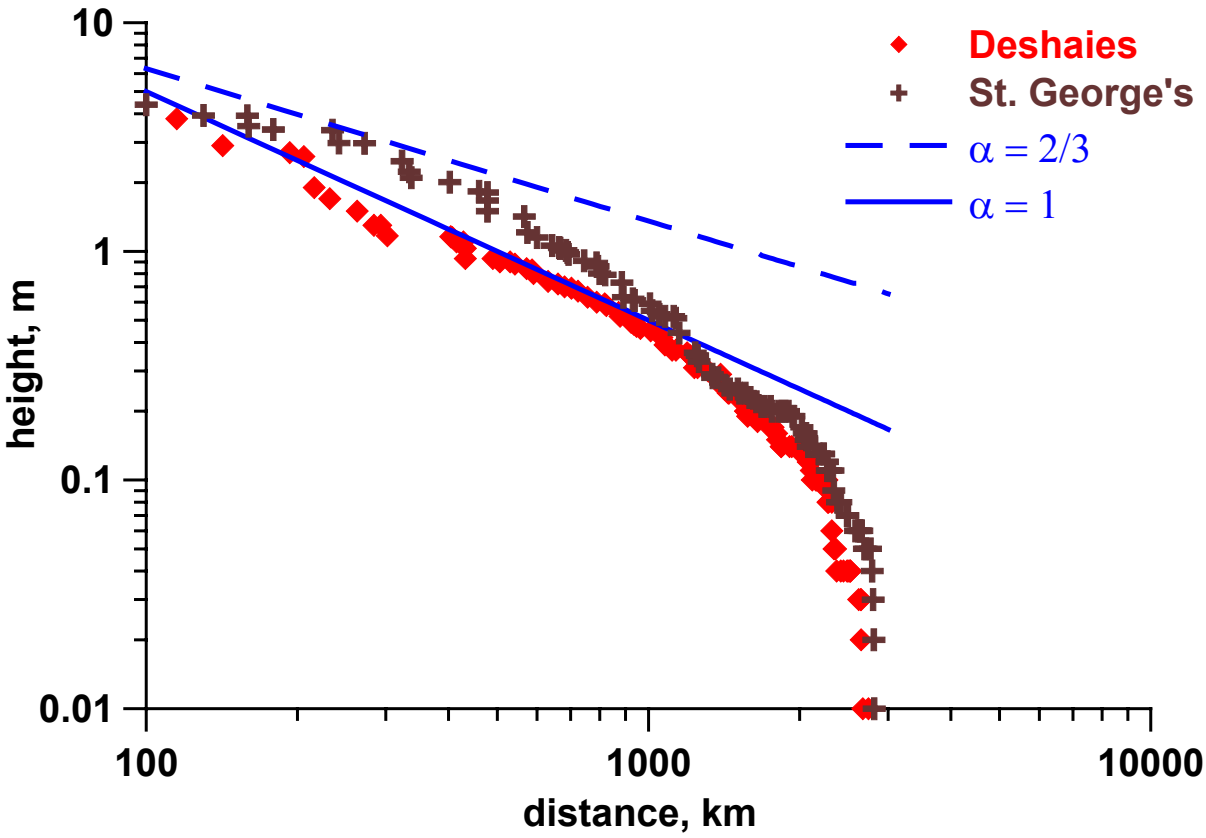

Figure 11. Computed tsunami height at Deshaies (Guadeloupe) and St. George's (Grenada) versus the distance to the source

6. Conclusion

The problem of evaluation of the far-field tsunami potential for the Caribbean Sea is discussed. Numerical simulation of the tsunami propagation from various hydrodynamics sources almost uniformly distributed along the coast of the Caribbean Sea and some seismic sources is performed in the framework of the nonlinear shallow-water equations by using the numerical code TUNAMI. The five zones with low tsunami risk with respect to the far-field tsunamis are selected in the Caribbean Sea. They are : Cuba (bay "Golfo de Batabano" and the coast of the province "Ciego de Avila"), Central America (near the border between Mexico and Belize, and the Nicaraguan coast between Bluefields and Puerto Cabezas) and the

Venezuelan coast (Bay "Golfo de Venezuela"). The analysis of historical tsunamis that occurred in the Caribbean Sea confirms that there was no tsunami in the computed zones of low tsunami risk. Also, the computing shows that the wave height is attenuated in an order if the tsunami source is located on distance about 1000 km from the coastal location, and such far-field tsunamis can be evaluated as low-risk tsunamis. The existence of zones with low tsunami risk with respect to the far-field tsunamis should be used for the planned tsunami warning system for the Caribbean Sea.

Acknowledgements. This study is supported by the grants from EGIDE (04500YH) and INTAS (01-2156), and for the Russian co-authors also by the grants from RFBR (02-05-6510 and 03-05-64975). The authors thank Professors Fumihiko Imamura and Ahmet Yalciner for the provided numerical code of TUNAMI.

References

Choi, B.H., Hong, S.J., and Pelinovsky, E. Simulation of prognostic tsunamis on the Korean coast, *Geophysical Research Letters*, 2001, vol. 28, 2013-2016.

Choi, B. H., Pelinovsky, E., Lee, J.S., and Woo, S.B. Estimation of tsunami risk zoning on the coasts adjacent to the East Coast from hypothetical earthquake, *J. Earthquake Engineering Society of Korea*, 2002a, vol. 6, 1-17.

Choi, B. H., Pelinovsky, E., Ryabov, I., and Hong, S.J. Distribution functions of tsunami wave heights, *Natural Hazards*, 2002b, vol. 25, 1-21.

Go, Ch.N., Kaistrenko, V.M., Pelinovsky, E.N., and Simonov, K.V. A Quantitative estimation of tsunami hazard and the tsunami zoning scheme of the Pacific Coast of the USSR, *Pacific Annual.* Vladivostok, 1988, 7–15.

Goto, C., Ogawa, Y., Shuto, N., and Imamura, N. Numerical method of tsunami simulation with the leap-frog scheme (IUGG/IOC Time Project), *IOC Manual*, UNESCO, No. 35, 1997.

Heinrich, F., Boudon, G., Komorowski, J.C., Sparks, R.S.J., Herd, R., and Voight, B. Numerical simulation of the December 1997 debris avalanche in Montserrat. *Geophys. Research Letters*, 2001, vol. 28, 2529-2532.

Heinrich, F., Guibourg, S., Mangeney, A., and Roche, R. Numerical modelling of a landslide-generated tsunami following a potential explosion of the Montserrat Volcano. *Phys. Chem. Earth*, 1999, vol. A24, 163-168.

Heinrich, F., Mangeney, A., Guibourg, S., and Roche, R. Simulation of water waves generated by a potential debris avalanche in Montserrat, Lesser Antilles. *Geophys. Research Letters*, 1998, vol. 25, 3697-3700.

HTDB/ATL *Expert Tsunami Database for the Atlantics*. Version 3.6 of March 15, 2002. Tsunami Laboratory, Novosibirsk, Russia, 2002.

Koike, N., Kawata, Y., and Imamura, F. Far-field tsunami potential and a real-time forecast system for the Pacific using the inversion method, *Natural Hazards*, 2003, vol. 29, 423-436.

Lander, J.F., Whiteside, L.S., and Lockridge, P.A. A brief history of tsunami in the Caribbean Sea. *Science of Tsunami Hazards*, 2002, vol. 20, 57-94.

Le Friant, A., Boudon, G., Komorowski, J-C., and Deplus, C. L'île de la Dominique, à l'origine des avalanches de débris les plus volumineuses de l'arc des Petites Antilles. *C.R. Geoscience*, 2002, vol. 334, 235-243.

Le Friant, A., Heinrich, P., Deplus, C., and Boudon, G. Numerical simulation of the last flank-collapse event of Montagne Pelée, Martinique, Lesser Antilles. *Geophys. Research Letters*, 2003, vol. 30, No. 2, 1034.

Mader, C.L. Modeling the 1755 Lisbon tsunami. *Science of Tsunami Hazards*, 2001a, vol. 9, 93-98.

Mader, C.L. Modeling the La Palma landslide tsunami. *Science of Tsunami Hazards*, 2001b, vol. 19, 150-170.

Mercado, A., and McCann, W. Numerical simulation of the 1918 Puerto Rico tsunami. *Natural Hazards*, 1998, vol. 18, 57-76.

Mercado, A., Grindlay, N., Lynett, P., and Liu, P.L.-F. Investigation of the potential tsunami hazard on the north coast of Puerto Rico due to submarine landslides along the Puerto Rico trench. 245p. Submitted to Puerto Rico State Emergency Management Agency. 2002.

Mofjeld, H.O., Titov, V.V., Gonzalez, F.I., and Newman, J.C. Tsunami scattering provinces in the Pacific Ocean, *Geophys. Research Letters*, 2001, vol. 28, 335-337.

Okada, Y. Surface deformation due to shear and tensile faults in a half-space, *Bull. Seism. Soc. America*, 1985, vol. 75, 1135-1154.

O'Loughlin, K.F., and Lander, J.F. *Caribbean Tsunamis: A 500-Year History from 1498–1998.* Advances in Natural and Technological Hazards Research, v. 20, Kluwer, 2003.

Nagano, O., Imamura, F., and Shuto, N. A numerical model for a far-field tsunamis and its application to predict damages done to aquaculture, *Natural Hazards*, 1991, vol. 4, 235-255.

Pararas-Carayannis, G. Evaluation of the threat of mega tsunami generation from postulated massive slope failures of island stratovolcanoes on La Palma, Canary Islands, and on the Island of Hawaii. *Science of Tsunami Hazards*, 2002, vol. 20, 251-277.

Sato, H., Murakami, H., Kozuki, Y., and Yamamoto, N. Study on a simplified method of tsunami risk assessment, *Natural Hazards*, 2003, vol. 29, 325-340.

Ward, S.N., and Day, S. Cumbre Vieja Volcano – potential collapse and tsunami at La Palma, Canary Islands. *Geophys. Research Letters*, 2001, vol. 28, 3397-3400.

Weissert, T.P. Tsunami travel time charts for the Caribbean. *Science of Tsunami Hazards*, 1990, vol. 8, 67-78.

Yalciner, A. C., Alpar, B., Altinok, T., Ozbay, I., and Imamura, F. Tsunamis in the Sea of Marmara. Historical documents for the past, models for the future. *Marine Geology*, 2002, vol. 190, 445-463.

Zahibo, N., and Pelinovsky, E. Evaluation of tsunami risk in the Lesser Antilles. *Natural Hazard and Earth Sciences*, 2001, vol. 3, 221-231.

Zahibo, N., Pelinovsky, E., and Kozelkov, A. The July 12, 2003 Montserrat tsunami. *Tsunami Newsletter*, 2003a (submitted).

Zahibo, N., Pelinovsky, E., Yalciner, A., Kurkin, A., Koselkov, A., and Zaitsev, A. The 1867 Virgin Island Tsunami: observations and modelling. *Oceanologica Acta*, 2003b, vol. 26, 609 – 621.